Alexandria Engineering Journal (2021) 60, 3219–3232

HOSTED BY

Alexandria University

Alexandria Engineering Journal

www.elsevier.com/locate/aej
www.sciencedirect.com

A hybrid fractional COVID-19 model with general population mask use: Numerical treatments

N.H. Sweilam [a,*], S.M. AL-Mekhlafi [b], A. Almutairi [c], D. Baleanu [d]

[a] Cairo University, Faculty of Science, Department of Mathematics, Giza, Egypt
[b] Sana'a University, Faculty of Education, Department of Mathematics, Yemen
[c] Department of Mathematics, Faculty of Science, University of Hafr AlBatin, Hafr AlBatin, Saudi Arabia
[d] Institute of Space Sciences, Magurele-Bucharest, Romania

Received 14 December 2020; revised 14 January 2021; accepted 29 January 2021
Available online 5 February 2021

KEYWORDS

Coronavirus diseases;
Face mask;
Hybrid fractional derivatives;
Compact finite difference method of six order;
Generalized fourth order Runge–Kutta method

Abstract In this work, a novel mathematical model of Coronavirus (2019-nCov) with general population mask use with modified parameters. The proposed model consists of fourteen fractional-order nonlinear differential equations. Grünwald-Letnikov approximation is used to approximate the new hybrid fractional operator. Compact finite difference method of six order with a new hybrid fractional operator is developed to study the proposed model. Stability analysis of the used methods are given. Comparative studies with generalized fourth order Runge–Kutta method are given. It is found that, the proposed model can be described well the real data of daily confirmed cases in Egypt.

1. Introduction

In present time the whole globe is facing a threatful outbreak called COVID-19 which originated from Wuhan; a large city in China. Since December 2019 to the 18th of July 2020, nearly 590,000 people died due to the mentioned disease and about 13.81 millions were all over the world. Also 7.718606 millions infected people have recovered from the disease, this data was recorded by WHO [1].

A novel coronavirus is a serious global issue and has a negative impact on the economy of Egypt. According to the publicly reported data, the first case of the novel corona virus in Egypt was reported on 14 February 2020. Total of 96753 cases were recorded in Egypt from the beginning of the pandemic until the eighteenth of August, where 96, 581 individuals were Egyptians and 172 were foreigners. The total number of people recovered reached 61, 562, or 63.6%, and the infection rate is 967 infectious per million of the population. The total number of deaths recorded 5, 184 deaths, of which 5, 165 were Egyptians, 19 were foreigners, and the death rate reached 5.3% of the infected.

* Corresponding author.
E-mail addresses: nsweilam@sci.cu.edu.eg (N.H. Sweilam), smdk100@gmail.com (S.M. AL-Mekhlafi), amalmutairi@uhb.edu.sa (A. Almutairi), dumitru@cankaya.edu.tr (D. Baleanu).

Peer review under responsibility of Faculty of Engineering, Alexandria University.

https://doi.org/10.1016/j.aej.2021.01.057

To understand the spread different infectious diseases including COVID-19 among plants, human or any other animals, mathematicians implement the concept of differentiation and integration to model the dynamics of that disease in the form of ODEs or PDEs that could be used to predict the transmission of that disease within a specific population. For this task, they divide the total population into different compartments. The solution of these systems may deliver an indication to health and other sectors that how severe the spread can be and what parameter is needed to control the spread of virus or disease under consideration.

Researchers around the world focus on the study the coronavirus infection in different scenarios. Some study the statistical tools to understand the infected cases and to find some relationships that can be used further to help the minimize the spread of the infection. Some studying the virus biologically and to think of some vaccine developments. Besides this, others develop mathematical models in terms to predict the infection eradication stage. Mathematical models are considered fast for many infectious diseases and its outbreak. Like corona infection, the authors used the theory of differential equations to formulate mathematical models with different characteristics and provided useful results for its eliminations. Several mathematical models are considered in literature in order to investigate and analyze the complex transmission pattern of the novel ongoing COVID-19 pandemic, see ([3–5,23,6–23,24–30,34]) and the references therein.

The fractional mathematical models that are generalized model and considered useful for modeling purposes in epidemiology. Various benefits can be obtained from a fractional order system in the sense of best data fitting, information about its memory and to identify the best possible value of the fractional order that can best describe the model for the real cases. In addition, the hereditary properties make the models constructed in fractional derivatives stronger and more useful for describing the real phenomenon [31]. It is useful than the ordinary order and with the benefit of crossover behaviors. Different mathematical models with interesting results are proposed in ([30] [13,17–20,21,22,35]–[36]) and the references therein. Moreover, it can be analyzed complex phenomena including disease models, see for example ([9,11,14–17,20,32,33]). One of the most effective and reliable operators is the hybrid fractional operator, it can be expressed as a linear combination of the Riemann–Liouville fractional integral and the Caputo fractional derivative. As in [5] this operator is general than Caputo fractional operator.

The analytic solution of such fractional order differential equations is difficult to be found. Hence, it is very important to develop numerical techniques to approximate the solutions of these models. High-order compact finite difference schemes are becoming increasingly common because of their high precision and the advantages associated with compact cells for more details see ([11,25]).

The aim of this work is to extend the model of COVID-19 with general population mask use which given as integer order in [3] to hybrid fractional order model and modified parameters. The boundedness, existence, uniqueness and the basic reproduction number of the present model will be discussed. Two high accuracy numerical methods are given to study the proposed model numerically. These methods are the compact finite difference of six order method with the Caputo proportional constant hybrid operator (CPC-CFD6M) and Generalized fourth order Runge–kutta method (GRK4M). Stability analysis of the used methods are given. Comparison between two methods will be given. We show that our COVID-19 model describes well the real data of daily confirmed cases in Egypt from 9 March to 13 June, 2020 [2].

To the best of our knowledge, the numerical studies using the high accuracy of compact finite difference of six order method for a hybrid fractional Coronavirus (2019-nCov) model with general population mask use and modified parameters have never been explored.

The rest of this paper is structured as follows: Preliminaries and notations are introduced in Section 2. The hybrid fractional order models are given and some properties of the proposed model such as the boundedness, existence, uniqueness and the basic reproduction number of the proposed model are proved in Section 3. Section 4, Numerical methods for solving the proposed model are presented. In Section 5, we discuss the numerical simulations. The conclusions are given in Section 6.

2. Background materials

In the following, some mathematical tools used in this work are introduced:

- We can define Caputo fractional order derivative as follows [4]:

$$ {}^{C}_{0}D^{\alpha}_{t}y(t) = \frac{1}{\Gamma(1-\alpha)}\int_{0}^{t} y\prime(s)(t-s)^{-\alpha}ds, \quad 0<\alpha<1, \tag{1} $$

  where Γ is the Euler gamma function.
- The Riemann–Liouville integral can be defined as follows [4]:

$$ {}^{RL}_{0}I^{\alpha}_{t}y(t) = \left[\int_{0}^{t} y(s)(t-s)^{\alpha-1}ds\right]\frac{1}{\Gamma(\alpha)}, \tag{2} $$

  where, $0<\alpha<1$ and $y(t)$ is an integrable function.
- The hybrid fractional operator is defined as follows [5]:

$$ {}^{CP}_{0}D^{\alpha}_{t}y(t) = \frac{1}{\Gamma(\alpha)}\left[\int_{0}^{t}(y(s)K_1(\alpha,s)+y\prime(s)K_0(\alpha,s))(t-s)^{-\alpha}ds\right], \tag{3} $$

  where, $K_0(\alpha,t)=\alpha t^{(1-\alpha)}$, $K_1(\alpha,t)=(1-\alpha)t^{\alpha}$, $0<\alpha<1$.

Definition 2.1. [5] The Caputo proportional hybrid operator (CP) given in (3) is defined either as general way:

$$ \begin{aligned} {}^{CP}_{0}D^{\alpha}_{t}y(t) &= \left(\int_{0}^{t}(y(s)K_1(s,\alpha)+y\prime(s)K_0(s,\alpha))(t-s)^{-\alpha}ds\right)\frac{1}{\Gamma(\alpha)}, \\ &= (K_1(t,\alpha)y(t)+K_0(t,\alpha)y\prime(t))\left(\frac{t^{\alpha}}{\Gamma(1-\alpha)}\right). \end{aligned} \tag{4} $$

Or as the Caputo proportional constant hybrid operator (CPC) [5]:

$$ \begin{aligned} {}^{CPC}_{0}D^{\alpha}_{t}y(t) &= \left(\int_{0}^{t}(t-s)^{-\alpha}(y(s)K_1(\alpha)+y\prime(s)K_0(\alpha))ds\right)\frac{1}{\Gamma(\alpha)} \\ &= K_1(\alpha)\,{}^{RL}_{0}I^{1-\alpha}_{t}y(t)+K_0(\alpha)\,{}^{C}_{0}D^{\alpha}_{t}y(t), \end{aligned} \tag{5} $$

where, $K_0(\alpha)=\alpha Q^{(1-\alpha)}$, $K_1(\alpha)=(1-\alpha)Q^{\alpha}$, Q is a constant.

Definition 2.2. The inverse operators to the fractional CPC derivatives is given by[5]:

$$ {}^{CPC}{}_0I_t^{\alpha}y(t) = \left(\int_0^t exp\left[\frac{K_1(\alpha)}{K_0(\alpha)}(t-s)\right] {}^{RL}{}_0D_t^{1-\alpha}y(s)ds\right)\frac{1}{K_0(\alpha)}. \quad (6) $$

3. Mathematical models of a hybrid fractional order

In the following, two Coronavirus spreading models with and without mask use which presented in [3] will be developed. We extended these models using a new hybrid fractional derivatives [5], moreover, the parameters dimensions will be adapted ([20,23]). These models given as follows:

3.1. A hybrid fractional order COVID-19 model without mask use

The hybrid fractional COVID-19 model without any mask use is given:

$$ \begin{aligned} {}^{CPC}{}_0D_t^{\alpha}S &= -\beta^{\alpha}(I+\eta A)\tfrac{S}{N},\\ {}^{CPC}{}_0D_t^{\alpha}E &= \beta^{\alpha}(I+\eta A)\tfrac{S}{N} - \sigma^{\alpha}E,\\ {}^{CPC}{}_0D_t^{\alpha}I &= \alpha_1\sigma^{\alpha}E - \phi I - \gamma_I^{\alpha}I,\\ {}^{CPC}{}_0D_t^{\alpha}A &= (1-\alpha_1)\sigma^{\alpha}E - \gamma_A^{\alpha}A,\\ {}^{CPC}{}_0D_t^{\alpha}H &= \phi^{\alpha}I - \delta^{\alpha}H - \gamma_H^{\alpha}H,\\ {}^{CPC}{}_0D_t^{\alpha}R &= \gamma_I^{\alpha}I + \gamma_A^{\alpha}A + \gamma_H^{\alpha}H,\\ {}^{CPC}{}_0D_t^{\alpha}D &= \delta^{\alpha}H. \end{aligned} \quad (7) $$

$$ R + E + I + S + A = N, $$

where, (E) denotes the exposed class, (I) denotes the symptomatic infectious class, (S) denotes the class of susceptible, (H) denotes the hospitalized class, (A) denotes the hospitalized asymptomatic infectious class, (R)denotes the recovered class and (D) denotes the cumulative deaths. Moreover, we assume that some fraction of symptomatic infectious individuals progress to the hospitalized class H are unable to pass the disease to the general public [3].

Table 1 The variables of system (8) and their definitions [3].

The abbreviation	Definition
R_U	Recovery class wears mask with uniform inward efficiency.
H_U	Hospitalized class wear masks with uniform inward efficiency.
E_U	Exposed class wear masks with uniform inward efficiency.
I_U	Infectious and symptomatic class wear masks with uniform inward efficiency.
S_U	Susceptible class wear masks with uniform inward efficiency.
D_U	Fatality class wear masks with uniform inward efficiency.
A_U	Infectious but asymptomatic class wear masks with uniform inward efficiency.
R_M	Recovery class wear general face mask.
H_M	Hospitalized class wear general face mask.
E_M	Exposed class wear general face mask.
I_M	Symptomatic and infectious class wear general face mask.
S_M	Susceptible class wear general face mask.
D_M	Fatality class wear general face mask.
A_M	Infectious but asymptomatic class wear general face mask.

3.2. A hybrid fractional COVID-19 model with general population mask use

In the following, we extended the COVID-19 model with general population mask use which given in [3] to a hybrid fractional order model with modified parameters. We consider the fractions of the general population wears masks outward efficiency and uniform inward. Let us consider U and M represent all population variables that typically do and do not wear masks, respectively. Both the variables and parameters of proposed models are given in Tables 1, 2 respectively. The hybrid COVID-19 multi-group fractional order model given as follows:

$$ \begin{aligned} {}^{CPC}{}_0D_t^{\alpha}S_U &= -\beta^{\alpha}(I_U+\eta A_U)\tfrac{S_U}{N} - \beta^{\alpha}(I_U(1-\varepsilon_0)+(1-\varepsilon_0)\eta A_U)\tfrac{S_U}{N},\\ {}^{CPC}{}_0D_t^{\alpha}E_U &= \beta^{\alpha}(I_U+\eta A_U)\tfrac{S_U}{N} + \beta^{\alpha}(I_U(1-\varepsilon_0)+(1-\varepsilon_0)\eta A_U)\tfrac{S_U}{N} - \sigma^{\alpha}E_U,\\ {}^{CPC}{}_0D_t^{\alpha}I_U &= \alpha_1\sigma^{\alpha}E_U - \phi I_U - \gamma_I^{\alpha}I_U,\\ {}^{CPC}{}_0D_t^{\alpha}A_U &= (1-\alpha_1)\sigma^{\alpha}E_U - \gamma_A^{\alpha}A_U,\\ {}^{CPC}{}_0D_t^{\alpha}H_U &= \phi^{\alpha}I_U - \delta^{\alpha}H_U - \gamma_H^{\alpha}H_U,\\ {}^{CPC}{}_0D_t^{\alpha}R_U &= \gamma_I^{\alpha}I_U + \gamma_A^{\alpha}A_U + \gamma_H^{\alpha}H_U,\\ {}^{CPC}{}_0D_t^{\alpha}D_U &= \delta^{\alpha}H_U, \end{aligned} $$

$$ \begin{aligned} {}^{CPC}{}_0D_t^{\alpha}S_M &= -\beta^{\alpha}(1-\varepsilon_i)(I_U+\eta A_U)\tfrac{S_M}{N} - \beta^{\alpha}(1-\varepsilon_i)(I_M(1-\varepsilon_0)+(1-\varepsilon_0)\eta A_M)\tfrac{S_M}{N},\\ {}^{CPC}{}_0D_t^{\alpha}E_M &= \beta^{\alpha}(1-\varepsilon_i)(I_U+\eta A_U)\tfrac{S_M}{N} + \beta^{\alpha}(1-\varepsilon_i)(I_M(1-\varepsilon_0)+(1-\varepsilon_0)\eta A_M)\tfrac{S_M}{N} - \sigma^{\alpha}E_M,\\ {}^{CPC}{}_0D_t^{\alpha}I_M &= \alpha_1\sigma^{\alpha}E_M - \phi^{\alpha}I_M - \gamma_I^{\alpha}I_M,\\ {}^{CPC}{}_0D_t^{\alpha}A_M &= (1-\alpha_1)\sigma^{\alpha}E_M - \gamma_A^{\alpha}A_M,\\ {}^{CPC}{}_0D_t^{\alpha}H_M &= \phi^{\alpha}I_M - \delta^{\alpha}H_M - \gamma_H^{\alpha}H_M,\\ {}^{CPC}{}_0D_t^{\alpha}R_M &= \gamma_I^{\alpha}I_M + \gamma_A^{\alpha}A_M + \gamma_H^{\alpha}H_M,\\ {}^{CPC}{}_0D_t^{\alpha}D_M &= \delta^{\alpha}H_M, \end{aligned} \quad (8) $$

$$ E_U + I_U + S_U + R_U + A_U + R_M + E_M + S_M + A_M + I_M = N. $$

Table 2 All parameters of systems (7) and (8) and their definitions.

Name	Definition	Value (per $day^{-\alpha}$)	Refrance
β^{α}	Infectious contact rate	2.5^{α}	Fitting
σ^{α}	Transition exposed to infectious	$(1/1.5)^{\alpha}$	[3]
η	Coefficient transmission due to super-spreaders	1.9 dimensionless	Fitting
α_1	A part of infections that will be symptomatic	0.5 dimensionless	[3]
ϕ	Rate of hospitalization	0.0025^{α}	[3]
γ^{α}	Recovery rate	$(1/7)^{\alpha}$	[3]
γ_A^{α}	Recovery rate, Asymptomatic	$(1/7)^{\alpha}$	[3]
γ_I^{α}	Recovery rate, symptomatic	$(1/7)^{\alpha}$	[3]
γ_H^{α}	Recovery rate, hospitalized	$(1/14)^{\alpha}$	[3]
δ^{α}	Rate of disease induced death of infected class	0.015^{α}	[3]

We can defined the feasible region for model (8) as follows:

$\Omega = \{(E_U, S_U, A_U, R_U, I_U, R_M, E_M, S_M, A_M, I_M) \in \mathbb{R}^{10}, E_U + I_U + S_U + R_U + A_U + R_M + E_M + S_M + A_M + I_M = N, \quad H_M, H_U, D_M, D_U \in \mathbb{R}^+\}$.

Boundedness of the proposed model solution can be verified by adding all equations of system (8) as follows:

$$D_{t\,0}^{\alpha\,CPC} N_g(t) = 0, \quad N_g(0) = A \geq 0, \tag{9}$$

where, A is a constant, N_g is total summation of population in system (8). The solution of (9) is given as follows [5]:

$$N_g(t) \geq A e^{(-\frac{K_1(\alpha)}{K_0(\alpha)} t)}, \tag{10}$$

It can be clearly seen from (10) at $t \longrightarrow \infty$, then $N_g(t) \geqslant 0$. Hence the solutions of the system (8) are bounded.

3.3. Existence and Uniqueness

In the following, we will use the fixed point theory. Let us rewrite (8)as follows:

$${}^{CPC}{}_0 D_t^{\alpha} y(t) = g(y(t), t), \quad y(0) = y_0 \geqslant 0. \tag{11}$$

The vector $y(t) = (E_U, H_U, D_U, S_U, A_U, R_U, I_U, R_M, E_M, H_M, D_M, S_M, A_M, I_M)^T$, represents the state variables and b is a continuous vector function such that:

$$\begin{pmatrix} g_1 \\ g_2 \\ g_3 \\ g_4 \\ g_5 \\ g_6 \\ g_7 \\ g_8 \\ g_9 \\ g_{10} \\ g_{11} \\ g_{12} \\ g_{13} \\ g_{14} \end{pmatrix} = \begin{pmatrix} -\beta^{\alpha}(I_U + \eta A_U)\frac{S_U}{N} - \beta^{\alpha}(I_U(1-\varepsilon_0) + (1-\varepsilon_0)\eta A_U)\frac{S_U}{N}, \\ \beta^{\alpha}(I_U + \eta A_U)\frac{S_U}{N} + \beta^{\alpha}(I_U(1-\varepsilon_0) + (1-\varepsilon_0)\eta A_U)\frac{S_U}{N} - \sigma^{\alpha} E_U \\ \beta^{\alpha}(I_U + \eta A_U)\frac{S_U}{N} + \beta^{\alpha}(I_U(1-\varepsilon_0) + (1-\varepsilon_0)\eta A_U)\frac{S_U}{N} - \sigma^{\alpha} E_U, \\ \alpha_1 \sigma^{\alpha} E_U - \phi I_U - \gamma_I^{\alpha} I_U \\ (1-\alpha_1)\sigma^{\alpha} E_U - \gamma_A^{\alpha} A_U \\ \phi^{\alpha} I_U - \delta^{\alpha} H_U - \gamma_H^{\alpha} H_U \\ \gamma_I^{\alpha} I_U + \gamma_A^{\alpha} A_U + \gamma_H^{\alpha} H_U \\ \delta^{\alpha} H_U \\ -\beta^{\alpha}(1-\varepsilon_i)(I_U + \eta A_U)\frac{S_M}{N} - \beta^{\alpha}(1-\varepsilon_i)(I_M(1-\varepsilon_0) + (1-\varepsilon_0)\eta A_M)\frac{S_M}{N} \\ \beta^{\alpha}(1-\varepsilon_i)(I_U + \eta A_U)\frac{S_M}{N} + \beta^{\alpha}(1-\varepsilon_i)(I_M(1-\varepsilon_0) + (1-\varepsilon_0)\eta A_M)\frac{S_M}{N} - \sigma^{\alpha} E_M \\ \alpha_1 \sigma^{\alpha} E_M - \phi^{\alpha} I_M - \gamma_I^{\alpha} I_M \\ (1-\alpha_1)\sigma^{\alpha} E_M - \gamma_A^{\alpha} A_M \\ \phi^{\alpha} I_M - \delta^{\alpha} H_M - \gamma_H^{\alpha} H_M \\ \gamma_I^{\alpha} I_M + \gamma_A^{\alpha} A_M + \gamma_H^{\alpha} H_M \\ \delta^{\alpha} H_M \end{pmatrix},$$

with initial condition y_0 Moreover, the Lipschitz condition is satisfied by g, where g is a quadratic vector function i.e. there exists $M^0 \in \mathbb{R}$, such that [26]:

$$\|g(y_1(t), t) - g(y_2(t), t)\| = M^0 \|y_1(t) - y_2(t)\|. \tag{12}$$

Theorem 3.1. The fractional proposed model (8) has unique solution if below condition holds:

$$\frac{M^0 \Upsilon_{max}^{\alpha} X_{max}^{\alpha}}{\Gamma(\alpha - 1) K_0(\alpha)} \leqslant 1. \tag{13}$$

Proof. We apply the definition (5) on (11), we get:

$$y(t) = y(t_0) + \frac{1}{K_0(\alpha)} \int_0^t exp(-\frac{K_1(\alpha)}{K_0(\alpha)}(t-s))^{RL}{}_0 D_t^{1-\alpha} g(y(s), s) ds. \tag{14}$$

Let $K = (0, T)$ and the operator $B : C(K, \mathbb{R}^{14}) \longrightarrow C(K, \mathbb{R}^{14})$such that:

$$B[y(t)] = y(t_0) + \frac{1}{K_0(\alpha)} \int_0^t exp(-\frac{K_1(\alpha)}{K_0(\alpha)}(t-s))^{RL}{}_0 D_t^{1-\alpha} g(y(s), s) ds. \tag{15}$$

It gives:

$B[y(t)] = y(t)$.

Let $\|.\|_K$ denotes the supremum norm on K. Thus

$\|y(t)\|_K = \sup_{t \in K} \|y(t)\|, \quad y(t) \in C(K, \mathbb{R}^{14})$.

So, $C(K, \mathbb{R}^{14})$ with $\|.\|_K$ is a Banach space. Moreover, the following relation holds:

$$\| \int_0^t \varphi(s,t) y(s) ds \| \leqslant \Lambda \|\varphi(s,t)\|_K \|y(s)\|_K,$$

with $y(t) \in C(K, \mathbb{R}^{14})$, $\varphi(s,t) \in C(K^2, \mathbb{R}^{14})$such that: $\|\varphi(s,t)\|_K = \sup_{t,s \in K} |\varphi(s,t)|$.Thus (15) can be written as:

$$\begin{aligned} &\|B[y_1(t)] - B[y_2(t)]\|_K \\ &\leqslant \| \tfrac{1}{K_0(\alpha)} \int_0^t exp(-\tfrac{K_1(\alpha)}{K_0(\alpha)}(t-s))(^{RL}{}_0 D_t^{1-\alpha} g(y_1(s), s) - {}^{RL}{}_0 D_t^{1-\alpha} g(y_2(s), s)) ds \|_K. \\ &\leqslant \tfrac{\Upsilon_{max}^{\alpha}}{\Gamma(\alpha-1) K_0(\alpha)} \| \int_0^t (t-s)^{\alpha-2} (g(y_1(s), s) - g(y_2(s), s)) ds \|_K, \\ &\leqslant \tfrac{\Upsilon_{max}^{\alpha} X_{max}^{\alpha}}{\Gamma(\alpha-1) K_0(\alpha)} \|g(y_1(t), t) - g(y_2(t), t)\|_K, \\ &\leqslant \tfrac{M^0 \Upsilon_{max}^{\alpha} X_{max}^{\alpha}}{\Gamma(\alpha-1) K_0(\alpha)} \|y_1(t) - y_2(t)\|_K. \end{aligned} \tag{16}$$

Finally, we obtain:

$$\|B[y_1(t)] - B[y_2(t)]\|_K \leqslant L \|y_1(t) - y_2(t)\|_K, \tag{17}$$

where

$$L = \frac{M^0 \Upsilon^{\alpha}_{max} X^{\alpha}_{max}}{\Gamma(\alpha-1)K_0(\alpha)}.$$

If $L \leqslant 1$, then the operator B is called a contraction. Hence, the fractional system (8) possesses a unique solution.

3.4. Basic reproduction number

We use the next generation method [6] to find the basic reproduction number. Consider the following matrices F and V, where F represents the new infection terms, V represents the remaining transfer terms [6]:

$$F = \begin{pmatrix} 0 & \beta_0^{\alpha}\frac{S_U(0)}{N(0)} & \beta_0^{\alpha}\eta\frac{S_U(0)}{N(0)} & 0 & \beta_0^{\alpha}(1-\epsilon_0)\frac{S_U(0)}{N(0)} & \beta_0^{\alpha}\eta(1-\epsilon_0)\frac{S_U(0)}{N(0)} \\ 0 & 0 & 0 & 0 & 0 & 0 \\ 0 & 0 & 0 & 0 & 0 & 0 \\ 0 & \beta_0^{\alpha}(1-\epsilon_i)\frac{S_M(0)}{N(0)} & \beta_0^{\alpha}\eta(1-\epsilon_i)\frac{S_M(0)}{N(0)} & 0 & \beta_0^{\alpha}(1-\epsilon_0)(1-\epsilon_i)\frac{S_M(0)}{N(0)} & \beta_0^{\alpha}\eta(1-\epsilon_0)(1-\epsilon_i)\frac{S_M(0)}{N(0)} \\ 0 & 0 & 0 & 0 & 0 & 0 \\ 0 & 0 & 0 & 0 & 0 & 0 \end{pmatrix},$$

$$V = \begin{pmatrix} \sigma^{\alpha} & 0 & 0 & 0 & 0 & 0 \\ -\alpha_1\sigma^{\alpha} & (\phi^{\alpha}+\gamma_I^{\alpha}) & 0 & 0 & 0 & 0 \\ -\sigma^{\alpha}(1-\alpha_1) & 0 & \gamma_A^{\alpha} & 0 & 0 & 0 \\ 0 & 0 & 0 & \sigma^{\alpha} & 0 & 0 \\ 0 & 0 & 0 & -\alpha_1\sigma^{\alpha} & (\phi^{\alpha}+\gamma_I^{\alpha}) & 0 \\ 0 & 0 & 0 & -\sigma^{\alpha}(1-\alpha_1) & 0 & \gamma_A^{\alpha} \end{pmatrix}.$$

Then,

$$R_0 = \rho(FV^{-1}) = \beta_0^{\alpha}\left[\frac{S_U(0)}{N(0)} + \frac{S_M(0)}{N(0)}(1-\varepsilon_0)(1-\varepsilon_i)\right]\left(\frac{\alpha_1}{\phi^{\alpha}+\gamma_I^{\alpha}} + \frac{\eta(1-\alpha_1)}{\gamma_A^{\alpha}}\right), \tag{18}$$

where, R_0 is the basic reproduction number of the model, and ρ indicates the spectral radius of FV^{-1}.

4. Numerical Methods

4.1. CPC-CFD6M

Let us consider the following fractional order differential equation:

$${}^{CPC}{}_0D_t^{\alpha}y(t) = f(t,y(t)), \quad 0 < \alpha \leqslant 1, \quad y(0) = y_0. \tag{19}$$

The first derivative approximation using the compact finite difference of six order method (CFD6M) is given as follows [10]:

$$y\prime(t_j) = \frac{1}{\tau}\left(\frac{-1}{60}y_{j-3} + \frac{9}{60}y_{j-2} - \frac{45}{60}y_{j-1} + \frac{45}{60}y_{j+1} - \frac{9}{60}y_{j+2} + \frac{1}{60}y_{j+3}\right) + O(\tau^6). \tag{20}$$

Now, we can discretize (19) using (20) and definition (5) with Grünwald-Letnikov approximation as follows:

$$\frac{K_1(\alpha)}{(\tau)^{\alpha-1}}\left(y_{j+1} + \sum_{i=1}^{j+1}\omega_i y_{j+1-i}\right) + \frac{K_0(\alpha)}{(\tau)^{\alpha}}\sum_{i=0}^{j+1}\mu_i\left[\frac{-1}{60}y_{j-i-3} + \frac{9}{60}y_{j-i-2} - \frac{45}{60}y_{j-i-1} + \frac{45}{60}y_{j-i+1} - \frac{9}{60}y_{j-i+2} + \frac{1}{60}y_{j-i+3} - q_i y(0)\right] = f(t_j,y_j), \tag{21}$$

where, $t^j = j\tau$, $\tau = \frac{T_f}{N_j}$, $N_j \in \mathbb{N}$, $\mu_i = (-1)^{i-1}\binom{\alpha}{i}$, $\mu_1 = \alpha$, $q_i = \frac{i^{\alpha}}{\Gamma(1-\alpha)}$ and $i = 1,2,\ldots,n+1$. $\omega_0 = 1, \omega_i = (1-\frac{\alpha}{i})\omega_{i-1}$. Additionally, consider [23]:

$$0 < \mu_{i+1} < \mu_i < \ldots < \mu_1 = \alpha < 1,$$

$$0 < q_{i+1} < q_i < \ldots < q_1 = \frac{1}{\Gamma(1-\alpha)}.$$

Put $C = \frac{K_1(\alpha)}{\tau^{\alpha-1}}$, $B = \frac{K_0(\alpha)}{\tau^{\alpha}}$ in (21). Then, we have:

$$y_{j+1} = \frac{1}{(\frac{45B}{60}+C)}\left(\left[f(t_j,y_j) + \frac{1}{60}y_{j-3} - \frac{9}{60}y_{j-2} + \frac{45}{60}y_{j-1} + \frac{9}{60}y_{j+2} - \frac{1}{60}y_{j+3}\right] - B\sum_{i=1}^{j+1}\mu_i\left[\frac{-1}{60}y_{j-i-3} + \frac{9}{60}y_{j-i-2} - \frac{45}{60}y_{j-i-1} + \frac{45}{60}y_{j-i+1} - \frac{9}{60}y_{j-i+2} + \frac{1}{60}y_{j-i+3} + q_i y(0)\right] - C\sum_{i=1}^{n+1}\omega_i y_{n+1-i}\right). \tag{22}$$

Remark 1. If $K_1(\alpha) = 0$ and $K_0(\alpha) = 1$ in (21), then we have the discretization of CFD6M with Caputo operator (C-CFD6M).

4.2. Stability of CPC-CFD6M

In order to investigate the stability of the proposed method 22 consider the test problem of linear fractional differential equation [24]:

$${}^{CPC}{}_0D_t^{\alpha}y(t) = \upsilon\, y(t), \quad t \in [0,T], \quad \alpha \in (0,1], \quad \upsilon < 0, \tag{23}$$

$$y(0) = y_0,$$

Using the approximation of CPC-CFD6M (22) we can discretize (23) as follows:

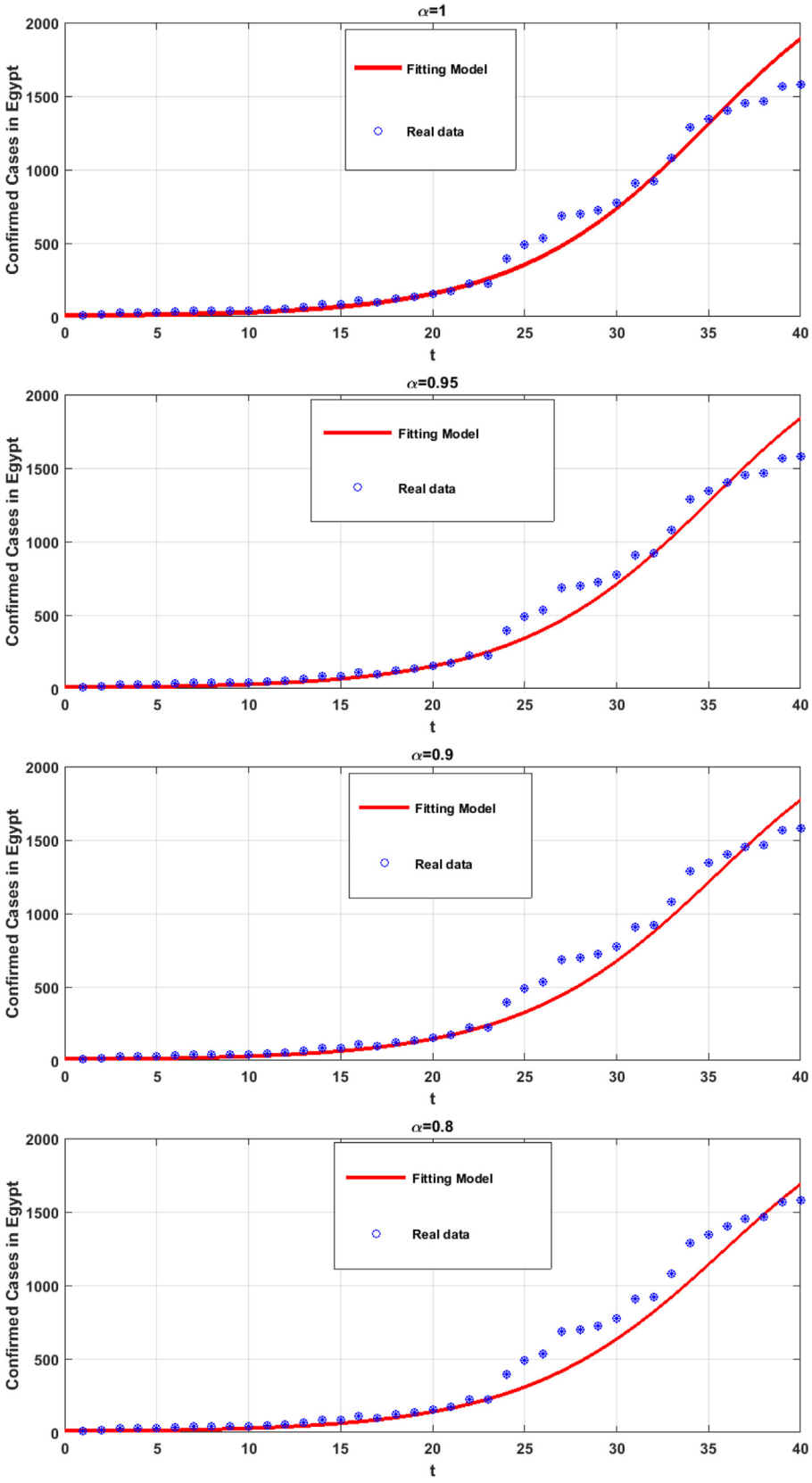

Fig. 1 Real data verses model (7) fitting at different α.

$$y_{j+1} = \frac{1}{(\frac{45B}{60}+C)}\Big(\big[\upsilon y(t_i) + \tfrac{1}{60}y_{j-3} - \tfrac{9}{60}y_{j-2} + \tfrac{45}{60}y_{j-1} + \tfrac{9}{60}y_{j+2} - \tfrac{1}{60}y_{j+3}\big] - B\sum_{i=1}^{j+1}\mu_i\big[\tfrac{-1}{60}y_{j-i-3} + \tfrac{9}{60}y_{j-i-2} - \tfrac{45}{60}y_{j-i-1} + \tfrac{45}{60}y_{j-i+1} - \tfrac{9}{60}y_{j-i+2} + \tfrac{1}{60}y_{j-i+3} + q_i y(0)\big] - C\sum_{i=1}^{n+1}\omega_i y_{n+1-i}\Big). \tag{24}$$

Then from boundness theorem [23] we have:

$$|y_{j+1}| = \frac{1}{(\frac{45B}{60}+C)}\Big|\big[\upsilon y(t_i) + \tfrac{1}{60}y_{j-3} - \tfrac{9}{60}y_{j-2} + \tfrac{45}{60}y_{j-1} + \tfrac{9}{60}y_{j+2} - \tfrac{1}{60}y_{j+3}\big] - B\sum_{i=1}^{j+1}\mu_i\big[\tfrac{-1}{60}y_{j-i-3} + \tfrac{9}{60}y_{j-i-2} - \tfrac{45}{60}y_{j-i-1} + \tfrac{45}{60}y_{j-i+1} - \tfrac{9}{60}y_{j-i+2} + \tfrac{1}{60}y_{j-i+3} + q_i y(0)\big] - C\sum_{i=1}^{n+1}\omega_i y_{n+1-i}\Big)\Big|. \tag{25}$$

Since, $(\frac{45B}{60}+C) > 1$, then we have: $|y_1| < |y_0|$ and $|y_0| \geqslant |y_1| \geqslant \ldots \geqslant |y_{n-1}| \geqslant |y_n| \geqslant |y_{n+1}|$. this means that, the proposed scheme is stable.

4.3. GRK4M

Consider the following FODE:

$${}^{C}_{0}D^{\alpha}_{t}y(t) = f(t, y(t)), \quad 0 < \alpha \leq 1, \quad 0 < t \leqslant T, \tag{26}$$

$y(0) = y_o$.

Then the approximate solution of (26) using GRK4M [7] is given as follows:

$$y_{n+1} = y_n + \frac{1}{6}(K_1 + 2K_2 + 2K_3 + K_4), \tag{27}$$

$$K_1 = \kappa f(t_n, y_n),$$

$$K_2 = \kappa f(t_n + \frac{1}{2}\kappa, y_n + \frac{1}{2}K_1),$$

$$K_3 = \kappa f(t_n + \frac{1}{2}\kappa, y_n + \frac{1}{2}K_2),$$

$$K_4 = \kappa f(t_n + \kappa, y_n + K_3),$$

where $\kappa = \frac{\tau^{\alpha}}{\Gamma(\alpha+1)}$.

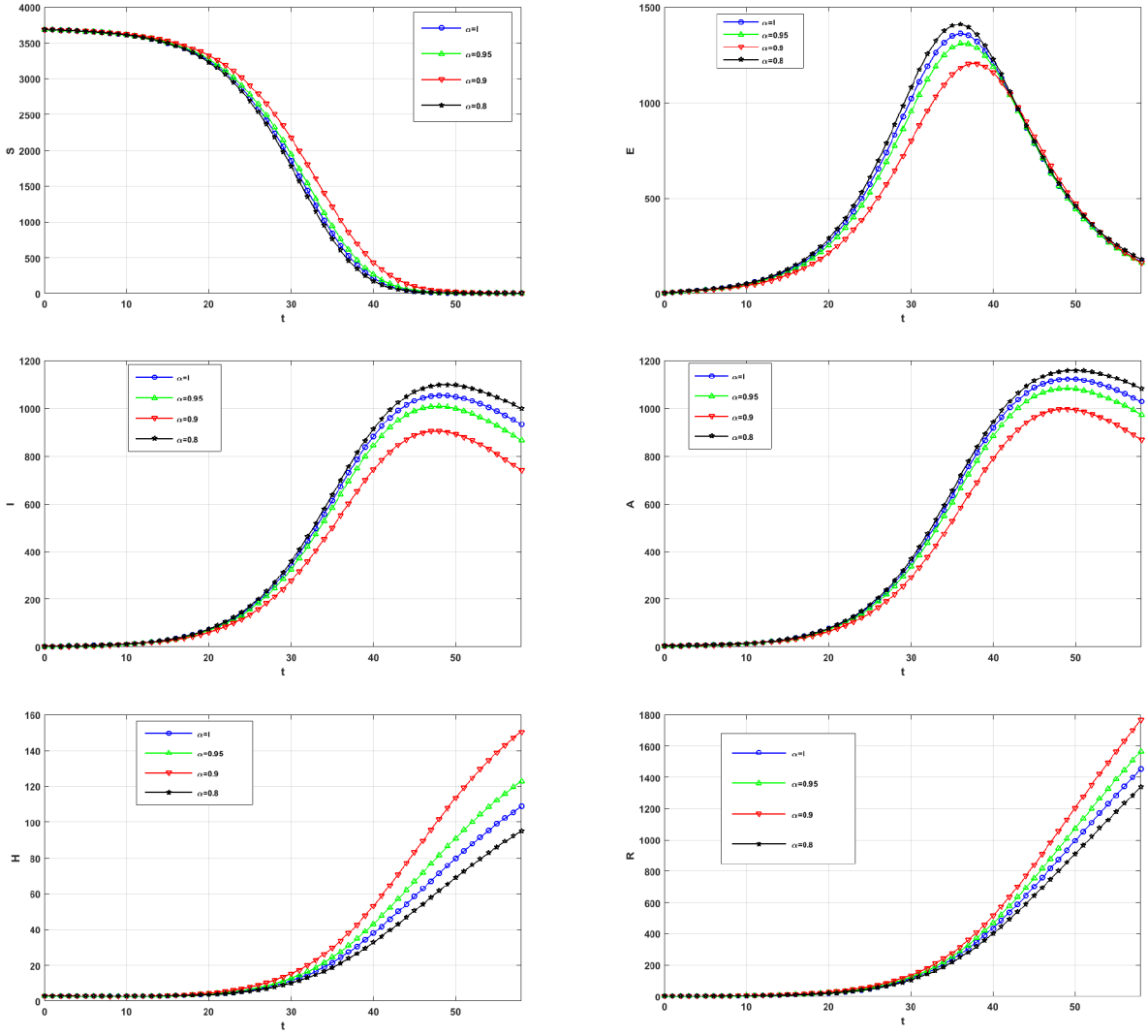

Fig. 2 Simulations of model (7) using at different values of α and $\beta = 2.5$ $\eta = 1.9$ using CPC-CFD6M.

4.4. Stability of GRK4M

In order to study the stability of GRK4M. Consider for simplicity the following test problem:

$$ {}^{C}{}_{0}D_{t}^{\alpha}y(t) = \upsilon\, y(t),\ \ 0 < t \leqslant T,\ \ \ 0 < \alpha \leq 1,\ \ \ \upsilon < 0, \tag{28} $$

$$ y(0) = y_o, $$

Using GRK4M [7], Eq. (28) can be written as follows:

$$ y(t_{j+1}) = y(t_j) + \frac{1}{6}\frac{\tau^{\alpha}\upsilon}{\Gamma(\alpha+1)}y(t_j),\ j = 0, 1, \ldots, n-1. \tag{29} $$

The stability analysis of GRK4M is similar to the GEM method [8], when the terms are regrouped, the following equation is achieved:

$$ y(t_{j+1}) = (1 + \frac{1}{6}\frac{\tau^{\alpha}\upsilon}{\Gamma(\alpha+1)})^{j} y_0,\ j = 0, 1, \ldots, n-1. \tag{30} $$

Then the stability condition [8] is given as follows:

$$ -1 < (1 + \frac{1}{6}\frac{\tau^{\alpha}\upsilon}{\Gamma(\alpha+1)}) < 1. $$

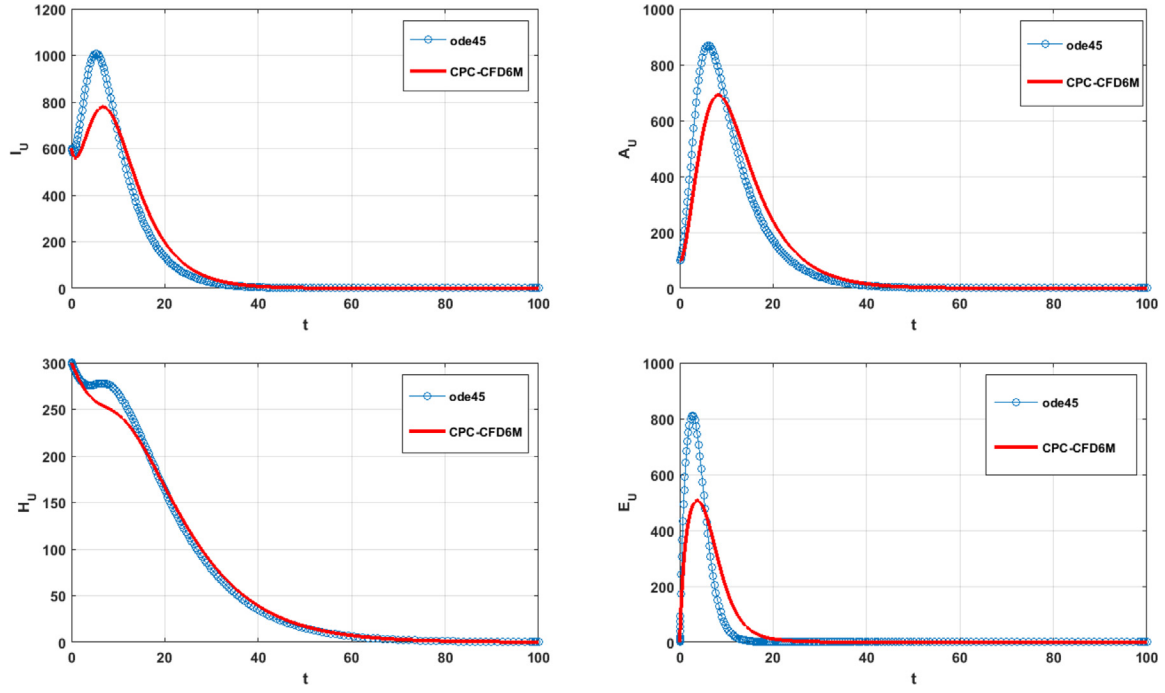

Fig. 3 Numerical simulations of E_U, I_U, A_U and H_U with and without mask use at $\alpha = 1$, $\beta = 0.5$ $\eta = 0.5$ using ode45 and CPC-CFD6M.

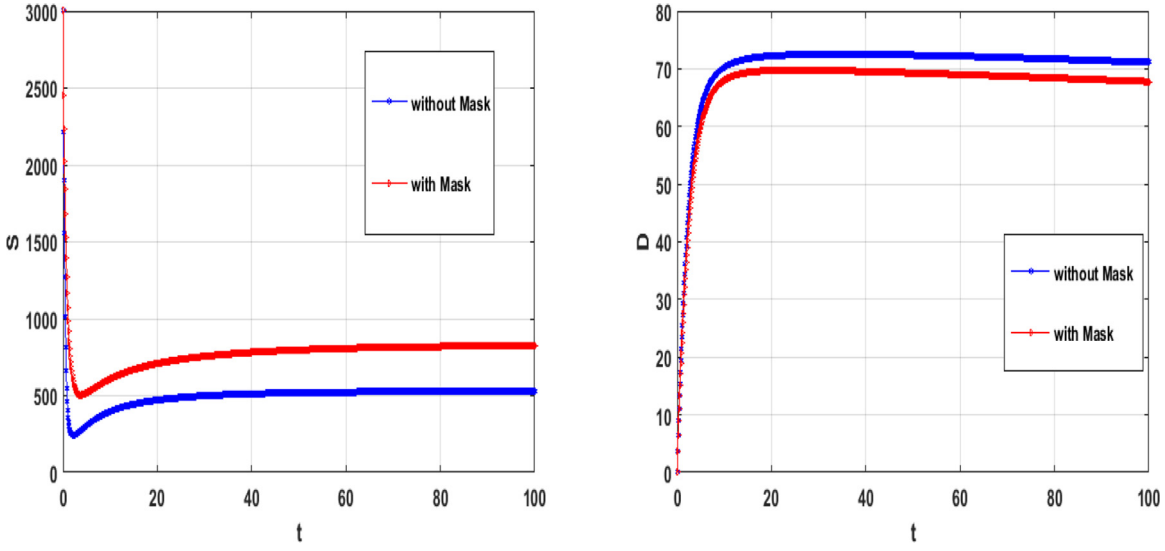

Fig. 4 Numerical simulations of S and D with and without mask use at $\alpha = 0.85$ using CPC-CFD6M.

5. Numerical experiments

In this section, CPC-NSFDM and GRK4M are constructed to obtain the numerical results of hybrid fractional models (7) and (8). For data fitting of model (7) we have taken some parameters values from the literature and the remaining values are fitted for the data collected for Egypt. We have fitted our model solutions with the real data collected from WHO for Egypt from 9th March 2020 to 13 June 2020 [2]. According to the publically reported data, the total population of Egypt for the year 2020 is 100500159. For the initial values we have considered $S(0) = (\frac{100500159}{27193}) - 10, I(0) = 2, E(0) = 0, A(0) = 5, H(0) = 3, R(0) = 0$ and $D(0) = 0$. We get different parameter values as shown in Table 2. This section provides graphical results of the given study. Fig. 1, shows the comparison between real data from WHO verses present considered model using CPC-CFD6M. It can be noted from this figure that the proposed model shows a strong agreement with real data collected by WHO. Fig. 2, depicts the influence of different values of parameter αon the dynamics and transmission of COVID-19 for different subclasses of the total population. In Figs. 3–10, simulations the model (8) at different values of the fractional order derivative, α, in the interval $(0, 1]$. The parameter values used in the simulations can be found in Table 2 and we put $\beta = 0.5, \eta = 0.5$ as given in [3]. The initial conditions are

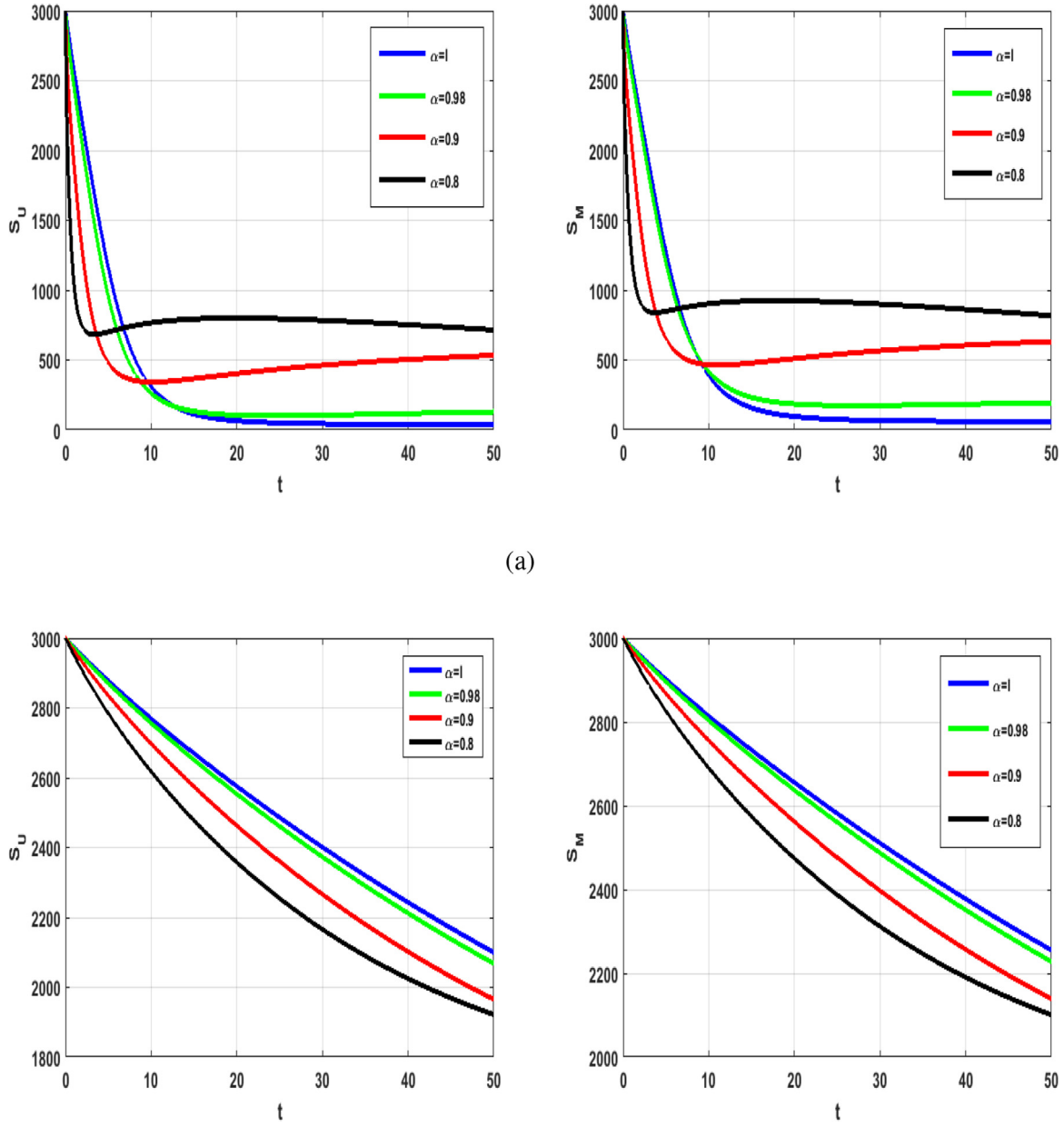

Fig. 5 Numerical simulations of S_U and S_M with mask use at different α using CPC-CFD6M in (a) and by using GRK4M in (b).

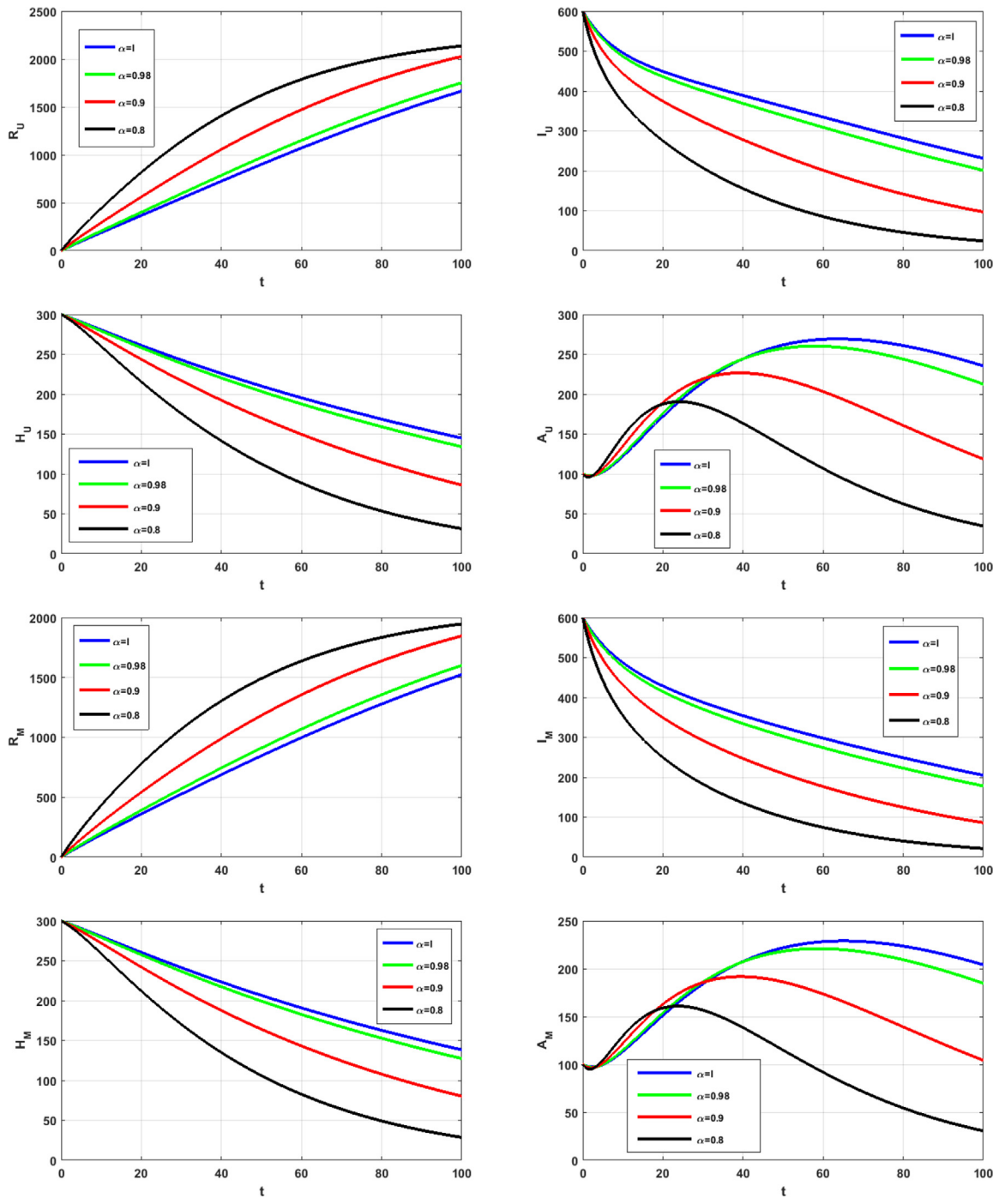

Fig. 6 Simulations of model (8) using GRK4 at different values of α.

set to $(3000, 0, 600, 100, 300, 0, 0, 3000, 0, 600, 100, 300, 0, 0)$. Fig. 3, shows the numerical solution of the model (8) using the Matlab solver ode45 and CPC-CFD6M at $\alpha = 1$, where the time levels are chosen in days. Fig. 4, illustrates the behavior of D and S with and without mask use at $\alpha = 0.96$ using CPC-CFD6M. We noted that, the number of susceptible individuals who use a mask is more than the number of susceptible individuals who do not use a mask. Also, the number of D who use a mask is less than the number of D who do not use a mask. Fig. 5, shows the numerical simulation of susceptible individuals who use a mask using CPC-CFD6M and GRK4M at differen values of α.

Fig. 6, shows the variables behavior of the model (8) at different value of α using GRK4M. Variables behavior of (8) are shown in Fig. 7, it changes with different values of α using CPC-CFD6M. Moreover, I_U, R_U and I_M, R_M behaviors are shown in Fig. 8, it changes when we use CPC-CFD6M and GRK4M. We noted that the number of I_U, I_M when we use CPC-CFD6M are less than the number of I_U when we use GRK4M. Also the number of R_U, R_M when we use CPC-

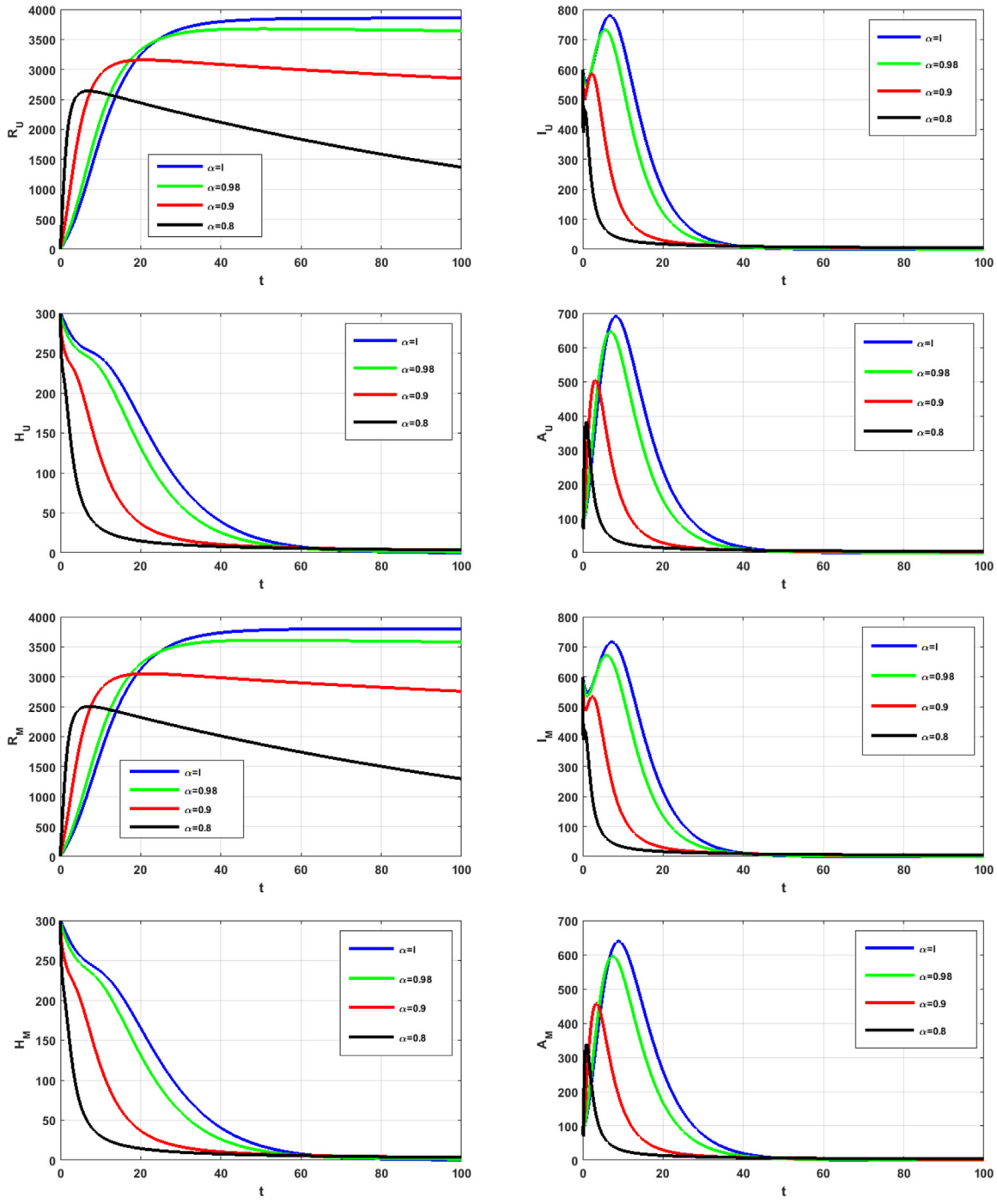

Fig. 7 Simulations of model (8) using CPC-CFD6M at different values of α.

CFD6M are more than the number of R_U, R_M when we use GRK4M. We can conclude that, CPC operator is preferable to simulate the biological models than the Caputo operator. We can obtain the Caputo operator as a spatial case from the new operator CPC when we put $K_0(\alpha) = 1$ and $K_1(\alpha) = 0$. Fig. 9, shows the numerical simulations of I_U and R_U at $\alpha = 0.9$ using C-CFD6M and GRK4M. We noted that results which obtain by C-CFD6M are better than the results which obtained by GRK4M. Also Fig. 10 shows how the behavior of I_U, A_U, H_U and I_M, A_M, H_M are changed with different values of α when we use C-CFD6M. Table 3 shows the CPU time for CPC-CFD6M and GRK4M. We noted that at $\alpha = 1$, the Matlab solver ode 45 is the fastest one, and for $0.8 < \alpha < 1$, GRK4M is faster than CPC-CFD6M.

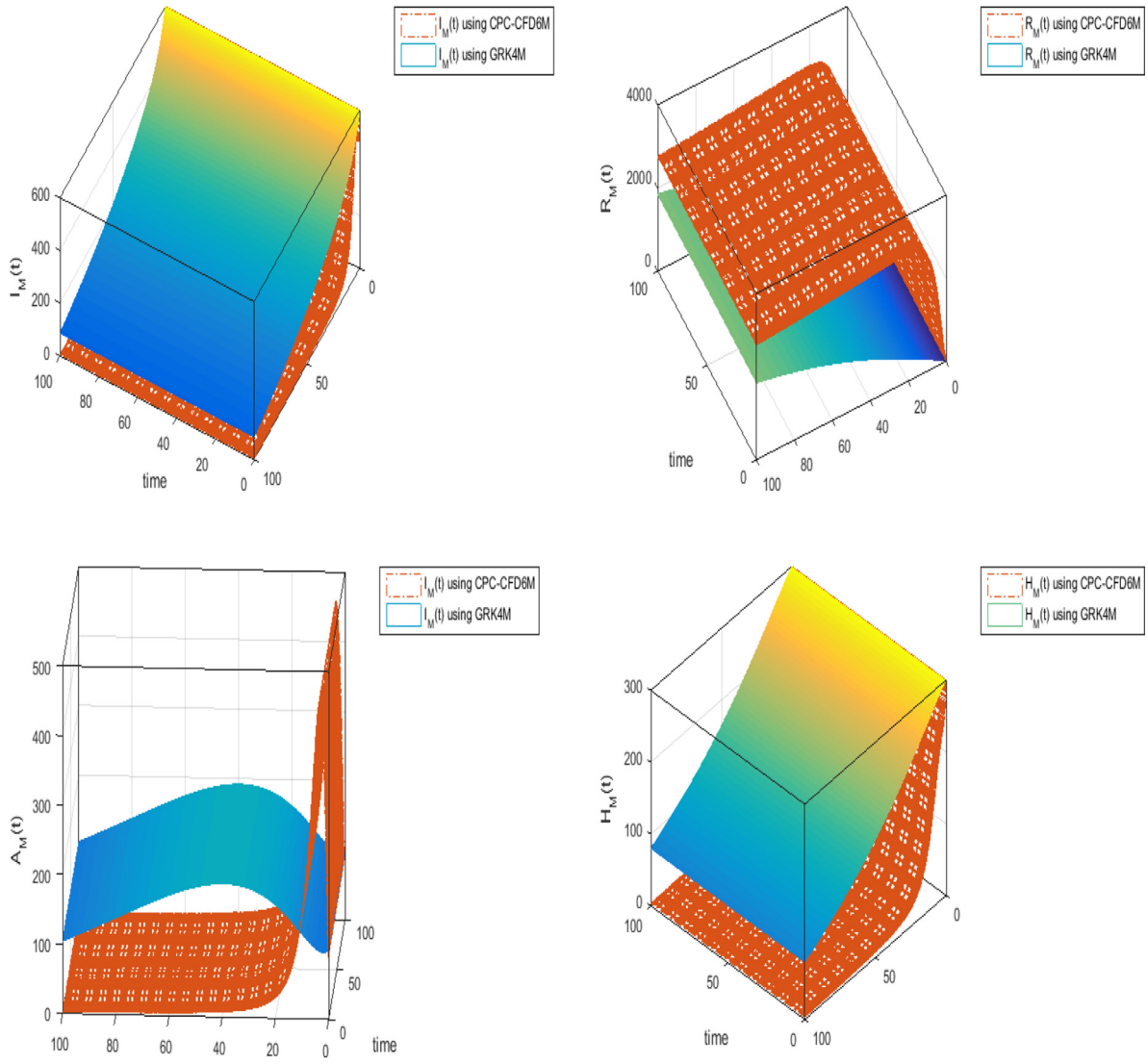

Fig. 8 Numerical simulations of I_M, A_M, H_M and R_M at $\alpha = 0.9$ using CPC-CFD6M and GRK4M.

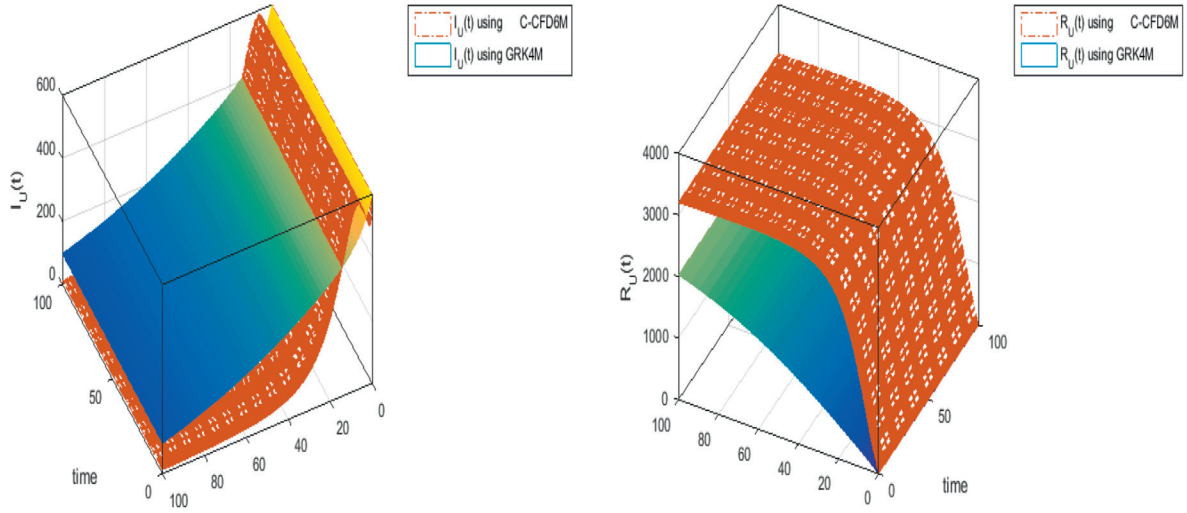

Fig. 9 Numerical simulations of I_U and R_U at $\alpha = 0.9$ using C-CFD6M and GRK4M.

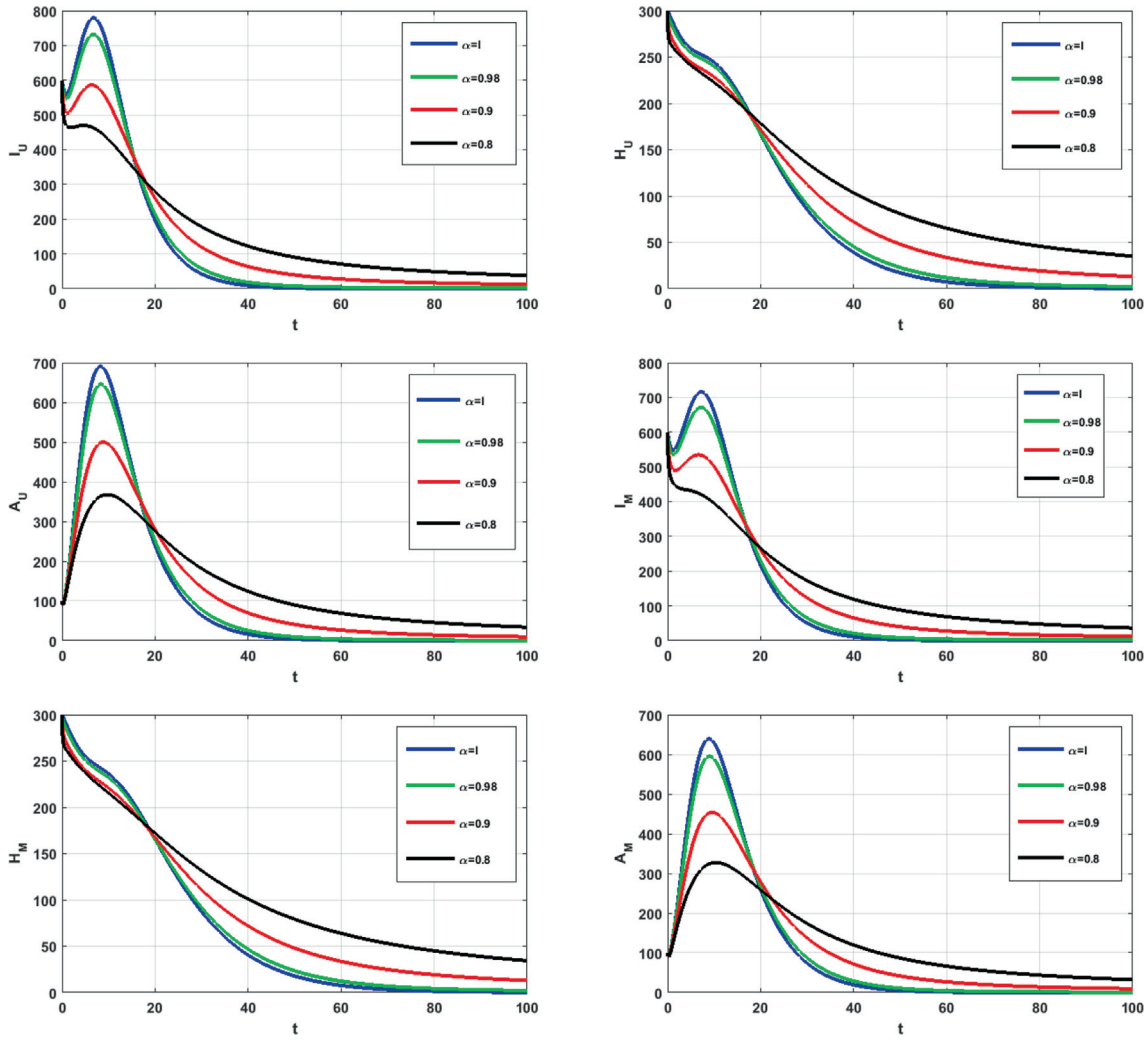

Fig. 10 Simulations of model (8) using C-CFD6M at different values of α.

Table 3 CPU time in seconds (CPUT) or the used methods at $T_f = 1000$.

α	CPUT of CPC-NSFDM	CPUT of GRK4M	CPUT of ode45
1	4.262203	2.701963	1.127760
0.98	4.166234	2.667243	–
0.90	4.157134	2.672843	–
0.80	4.233840	2.658462	–

6. Conclusions

In this article a novel hybrid fractional COVID-19 model with general population mask use and modified parameters is presented. This fractional model can be described the phenomena with memory than the integer order model. Also, the model in [3] can be obtained as a special case from the proposed model when $\alpha = 1$. We can conclude from the obtained results in this work that, the proposed COVID-19 model describes well the real data collected by WHO [1] of daily confirmed cases in Egypt. Existence, uniqueness and boundedness of the solutions are proved, moreover, the basic reproduction number is discussed. Two highly accurate numerical methods are used to study the presented model. These methods are GRK4M and CPC-CFD6M. Mathematical analysis for GRK4M and CPC-CFD6M are introduced. Comparative studies are done and we can conclude from Table 3 and the graphical results that the CPC-CFD6M is prefable to describe the biological results than the GRK4M, but GRK4M is faster than the CPC-CFD6M. Moreover, Caputo operator can be obtained as a special case from the new hyprid operator CPC.

Declaration of Competing Interest

None.

Acknowledgments

This work was supported by the Cairo university, Coronavirus (2019-nCov) projects, project No. 1, and the authors acknowledge this support.

References

[1] World Health Organization. Coronavirus. World Health Organization, cited January 19, 2020. Available: https://www.who.int/health-topics/coronavirus.

[2] WHO Coronavirus Disease (COVID-19), Egypt, https://covid19.who.int/table.

[3] S.E. Eikenberry, M. Mancuso, E. Iboi, T. Phan, K. Eikenberry, Y. Kuang, E. Kostelich, A. Gumel, To mask or not to mask: Modeling the potential for face mask use by the general public to curtail the COVID-19 pandemic, Infectious Disease Model. 2 (2020) 293–308.

[4] I. Podlubny, Fractional Differential Equations, Academic Press, New York, 1999.

[5] D. Baleanu, A. Fernandez, A. Akgül, On a fractional operator combining proportional and classical differintegrals, Mathematics 8 (3) (2020), https://doi.org/10.3390/math8030360.

[6] P. Driessche, P. Watmough, Reproduction numbers and sub-threshold endemic equilibria for compartmental models of disease transmission, Math. Biosci. 180 (2002) 29–48.

[7] C. Milici, J.T. Machado, G. Draganescu, Application of the Euler and Runge-Kutta generalized methods for FDE and symbolic packages in the analysis of some fractional attractors, Int. J. Nonlinear Sci. Numer. Simul. 21 (2) (2019).

[8] N.H. Sweilam, S.M. AL-Mekhlafi, Optimal control for a nonlinear mathematical model of tumor under immune suppression: a numerical approach, Optim. Control Appl. Meth. 39 (5) (2018) 1581–1596, https://doi.org/10.1002/oca.2427.

[9] W. Lin, Global existence theory and chaos control of fractional differential equations, JMAA 332 (2007) 709–726.

[10] K.M. Owolabi, A. Atangana, Numerical methods for fractional differentiation, Springer Series Comput. Math. (54) (2019), https://doi.org/10.1007/978-981-15-0098-5.

[11] N.H. Sweilam, S.M. Al-Mekhlafi, A.O. Albalawi, Optimal control for a fractional order malaria transmission dynamics mathematical model, Alexandria Eng. J. 59 (2020) 1677–1692, https://doi.org/10.1016/j.aej.2020.04.020.

[12] N.H. Sweilam, S.M. AL-Mekhlafi, D. Baleanu, A hybrid fractional optimal control for a novel Coronavirus (2019-nCov) mathematical model, J. Adv. Res., (2020), DOI: 10.1016/j.jare.2020.08.006.

[13] F. Ndäirou, I. Area, J.J. Nieto, D.F.M. Torres, Mathematical modeling of COVID-19 transmission dynamics with a case study of Wuhan, Chaos, Solitons Fract. (2020), https://doi.org/10.1016/j.chaos.2020.109846.

[14] A. Carvalho, C. Pinto, J. de Carvalho, Mathematical Modelling and Optimization of Engineering Problems, Springer, Cham, 2020, pp. 175–185.

[15] C. Pinto, A. Carvalho, Fractional dynamics of an infection model with time-varying drug exposure, J. Comput. Nonlinear Dyn. 13 (19) (2018), https://doi.org/10.1115/1.4038643.

[16] S. Kumar, R. Kumar, J. Singh, K. Nisar, D. Kumar, An efficient numerical scheme for fractional model of HIV-1 infection of CD4+ T-cells with the effect of antiviral drug, therapy, Alexandria Eng. J. 59 (2020) 2053–2064.

[17] K.M. Safare, V.S. Betageri, D.G. Prakasha, P. Veeresha, S. Kumar, A mathematical analysis of ongoing outbreak COVID-19 in India through nonsingular derivative, Numer. Methods Partial Differential Eq. (2020) 1–17, https://doi.org/10.1002/num.22579.

[18] M.A. Khan, A. Atangana, E. Alzahrani, F. Fatmawati, The dynamics of COVID-19 with quarantined and isolation, Adv. Difference Eqs. (2020), https://doi.org/10.1186/s13662-020-02882-9.

[19] N.H. Sweilam, S.M. AL-Mekhlafi, A.O. Albalawi, D. Baleanu, On the Optimal Control of Coronavirus (2019-nCov) Mathematical Model; A Numerical Approach, Advances in Difference Equations, 528, (2020), doi: 10.1186/s13662-020-02982-6.

[20] M. Hajipour, A. Jajarmi, D. Baleanu, An efficient nonstandard finite difference scheme for a class of fractional chaotic systems, J. Comput. Nonlinear Dyn. 13 (2018) 1–9, https://doi.org/10.1115/1.4038444.

[21] M.A. Khan, A. Atangana, Modeling the dynamics of novel coronavirus (2019-nCov) with fractional derivative, Alex. Eng. J. 59 (2020) 2379–2389, https://doi.org/10.1016/j.aej.2020.02.033.

[22] J.A.T. Machado, A.M. Lope, Rare and extreme events: the case of COVID-19 pandemic, Nonlinear Dyn. 16 (2020) 1–20.

[23] A.J. Arenas, G. Gonzàlez-Parra, B.M. Chen-Charpentierc, Construction of nonstandard finite difference schemes for the SI and SIR epidemic models of fractional order, Math. Comput. Simul. 121 (2016) 48–63.

[24] F.A. Rihan, D. Baleanu, S. Lakshmanan, R. Rakkiyappan, On fractional SIRC model with Salmonella bacterial infection, Abstract Appl. Anal. 1–9 (2014).

[25] J.W. Thomas, Numerical Partial Differential Equations: Finite Difference Methods, Springer, 1998.

[26] E. Bonyah, A.K. Sagoe, D. Kumar, S. Deniz, Fractional optimal control dynamics of Coronavirus model with Mittag-Leffler law, Ecol. Compl. 45 (2020) 100880, https://doi.org/10.1016/j.ecocom.2020.100880.

[27] A.S. Shaikh, I.N. Shaikh, K.S. Nisar, A mathematical model of COVID-19 using fractional derivative: outbreak in India with dynamics of transmission and control, Adv. Differ. Equ. 373 (2020).

[28] O.J. Peter, A.S. Shaikh, M.O. Ibrahim, K.S. Nisar, D. Baleanu, I. Khan, A.I. Abioye, Analysis and dynamics of fractional order mathematical model of COVID-19 in Nigeria using Atangana-Baleanu operator, Comput., Mater. Continua 66 (2) (2021) 1823–1848.

[29] Z. Ahmad, M. Arif, F. Ali, I. Khan, K.S. Nisar, A report on COVID-19 epidemic in Pakistan using SEIR fractional model, Scient. Rep. 10 (1) (2020), https://doi.org/10.1038/s41598-020-79405-9.

[30] C. Ravichandran, K. Logeswari, F. Jarad, New results on existence in the framework of Atangana-Baleanu derivative for fractional integro-differential equations, Chaos, Solitons and Fractals 125 (2019) 194–200.

[31] S. Kumar, R.P. Chauhan, S. Momani, S. Hadid, Numerical investigations on COVID-19 model through singular and non-singular fractional operators, Numer. Methods Partial Differ. Eq. (2020) 1–27, https://doi.org/10.1002/num.22707.

[32] P.A. Naik, K.M. Owolabi, M. Yavuz, J. Zu, Chaotic dynamics of a fractional order HIV-1 model involving AIDS-related cancer cells, Chaos, Solitons and Fractals 140 (2020) 110272.

[33] P.A. Naik, M. Yavuz, J. Zu, The role of prostitution on HIV transmission with memory: A modeling approach, Alexandria Eng. J. 59 (2020) 2513–2531.

[34] P.A. Naik, M. Yavuz, S. Qureshi, J. Zu, S. Townley, Modeling and analysis of COVID-19 epidemics with treatment in fractional derivatives using real data from Pakistan, Eur. Phys. J. Plus 135 (2020) 795.

[35] M. Yavuz, T. Abdeljawad, Nonlinear regularized long-wave models with a new integral transformation applied to the fractional derivative with power and Mittag-Leffler kernel, Adv. Differ. Equ. 367 (2020), https://doi.org/10.1186/s13662-020-02828-1.

[36] M. Yavuz, European Option Pricing Models Described by Fractional Operators with Classical and Generalized Mittag-Leffler Kernels, Numer. Methods Partial Differential Equ. (2020), https://doi.org/10.1002/num.22645.